New Journal of Physics
The open access journal at the forefront of physics
Deutsche Physikalische Gesellschaft DPG | IOP Institute of Physics

Magnetic ghosts and monopoles

N Vandewalle[1] **and S Dorbolo**
GRASP, Université de Liège, B-4000 Liège, Belgium
E-mail: nvandewalle@ulg.ac.be

Received 8 October 2013, revised 13 December 2013
Accepted for publication 8 January 2014
Published 30 January 2014
New Journal of Physics **16** (2014) 013050
doi:10.1088/1367-2630/16/1/013050

Abstract
While the physics of equilibrium systems composed of many particles is well known, the interplay between small-scale physics and global properties is still a mystery for athermal systems. Non-trivial patterns and metastable states are often reached in those systems. We explored the various arrangements adopted by magnetic beads along chains and rings. Here, we show that it is possible to create mechanically stable defects in dipole arrangements keeping the memory of dipole frustration. Such defects, nicknamed 'ghost junctions', seem to act as macroscopic magnetic monopoles, in a way reminiscent of spin ice systems.

1. Introduction

Neodyme sphere magnets are a beloved puzzle for geeks. Since dipole–dipole interactions are stronger than the weight of the beads, stable structures such as chains (one-dimensional (1D)), hexagons (two-dimensional (2D)) and cubic lattices (three-dimensional (3D)) can be easily created. Figure 1(a) presents a cube composed by 216 beads. Following tips and tricks, complex 3D structures can be also built from icosahedra to fractal Sierpinsky pyramids. Of course, the key ingredient of stability for these structures is the dipole–dipole interaction that one can find in physics systems at all scales.

At the microscopic scale, models considering dipole ordering are introduced in the case of equilibrium systems [1] for capturing the various magnetic phases that one may encounter in material science. The case of magnetic colloids [2, 3], where thermal agitation and dipole–dipole interaction compete, has also been extensively studied. The magnetic particles are known to

[1] Author to whom any correspondence should be addressed.

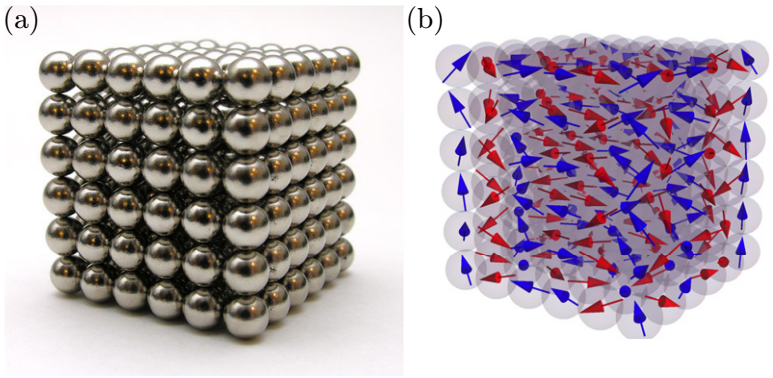

Figure 1. (a) A popular puzzle: a cube of 6^3 magnetized beads. (b) Dipole ordering in the cube as obtained from our numerical simulations based on the minimization of total energy U. Blue and red colours are used to distinguish upward/downward orientations of the dipoles along the vertical axis.

form chains and rings [4], the latter being broken by an external field [5]. It has been also shown that the thermalization of the particles can also be performed by using ac external fields [6, 7].

At a mesoscopic scale, thermal agitation is dominated by magnetic interactions. Dipole–dipole interactions are proposed to generate self-assembled structures [8–12]. When placed at a liquid interface, magnetic particles self-assemble into clusters of chains, crystals and loops [13] without any agitation. The presence of an external field is able to control these dissipative structures [12, 14]. The case of macroscopic athermal dipoles was however poorly explored. Only a few experiments were performed in order to study the various configurations adopted by a collection of magnetized beads. In a pioneering study, Blair and Kudrolli [15] realized series of experiments onto a vibrating plate, injecting mechanical energy into the system: chains, rings and 2D crystals have been observed. Lumay and Vandewalle [16] explored the properties of a granular packing submitted to a vertical magnetic field: the beads are organized such that low packing fractions can be reached. In another experiment, Carvente *et al* [17] obtained denser self-assembled systems using magnetized spheres. In the dilute limit, Falcon *et al* [18] experimented random magnetic forcing of a granular gas.

The main motivation of this work is to explore the possible dipole configurations adopted by a collection of magnetized spheres. A series of fundamental questions arises: What is the link between the stability of an assembly composed of several magnetic beads and the dipole orientations? Do different (metastable) states exist? We performed several experiments with magnetized beads and we rationalized results using numerical simulations. In this paper, we present the striking results obtained with apparent simple systems. The most relevant one is the obtention of monopole-like behaviours.

2. Chains

As found in classical textbooks [19], uniformly magnetized spheres behave like dipoles. The interaction energy between two point-like dipoles $\vec{m}_i$ and $\vec{m}_j$ is given by

$$u_{ij} = \frac{\mu_0}{4\pi}\left[\frac{\vec{m}_i \cdot \vec{m}_j}{r_{ij}^3} - 3\frac{(\vec{m}_i \cdot \vec{r}_{ij})(\vec{m}_j \cdot \vec{r}_{ij})}{r_{ij}^5}\right], \tag{1}$$

where $\vec{r}_{ij} = \vec{r}_j - \vec{r}_i$ is the vector linking particles i and j. We consider identical beads such that they have similar sizes and similar magnetizations ($|\vec{m}_i| = m$). It is therefore possible to define a dimensionless macroscopic potential as

$$U = \frac{2\pi D^3}{\mu_0 m^2} \sum_{i \neq j} u_{ij}, \tag{2}$$

where D is the sphere diameter and m being the bead moment. The algorithm used in our work consider the positions (x_i, y_i, z_i) and angular orientations (θ_i, φ_i) of each dipole i. In order to explore different structures, the sphere positions are fixed while the orientation of dipoles are free parameters. The algorithm starts from a random orientations of the spins and searches iteratively for the minimum of energy by changing slightly the angles θ_i and φ_i. As a first example, figure 1(b) proposes one of the low energy configurations for the spins arranged in a cube. Colours indicate different dipole orientations along the vertical axis. A complex ordering is found inside the cube. Along the main axes of the cube, chains of dipoles having similar orientations are found. Moreover, helicoidal-like orientations are also observed. Since 3D structures show complex dipole ordering, we first focused on chains of magnetic beads, as shown in figure 2(a). Chains are known to represent the natural way magnetic particles self-assemble. Indeed, the interaction given by equation (1) is highly anisotropic, and strong attractive interactions are obtained for aligned dipoles [20]. By searching the minimization of energy of the dipoles, the ground state is found to be a simple alignment of the dipoles along the chain, as shown in figure 2(a). One has

$$U_0 = -2 \sum_{i=1}^{N-1} \frac{(N-i)}{i^3}. \tag{3}$$

From that pattern, the continuous deformation of a chain towards a ring configuration will emphasize the transition seen in [15]. The chain is slightly deformed such that it forms an arc with a cumulated angle α. When α reaches 360°, a ring is formed. The radius of curvature of the chain is therefore $R = ND/\alpha$. From numerical simulations, figure 2(b) shows the energy per dipole U/N as a function of α for different chain sizes N. Two minima are seen in the curves at $\alpha = 0$ (chain) and $\alpha = 360°$ (ring) respectively. They are separated by an energy barrier, whose maximum is around $\alpha_{\max} \approx 280°$ for large N values. This energy barrier can be tested experimentally. For finite systems (and for $N > 3$), the ring configuration is more stable than the chain. This explains why rings were often observed in Blair and Kudrolli [15] experiments. When the bead number increases, the barrier seems to vanish. Since the energy of an infinite chain is expected to coincide with the energy of the infinite ring, the energy per particle decreases towards an asymptotic value U_∞/N whatever the angle α. This asymptotic value can be evaluated by

$$\frac{U_\infty}{N} = \lim_{N \to \infty} \frac{U_0}{N} = -2\zeta(3) \approx -2.404, \tag{4}$$

where ζ is the Riemann zeta function. The major feature of the energy landscapes presented in figure 2(b) is the presence of an energy barrier whose angular position $\alpha_{\max}$ is marginally sensitive to N. One would expect that the ring will form when the interaction between both extremities of the chain reaches high values, i.e. when they are close to each other.

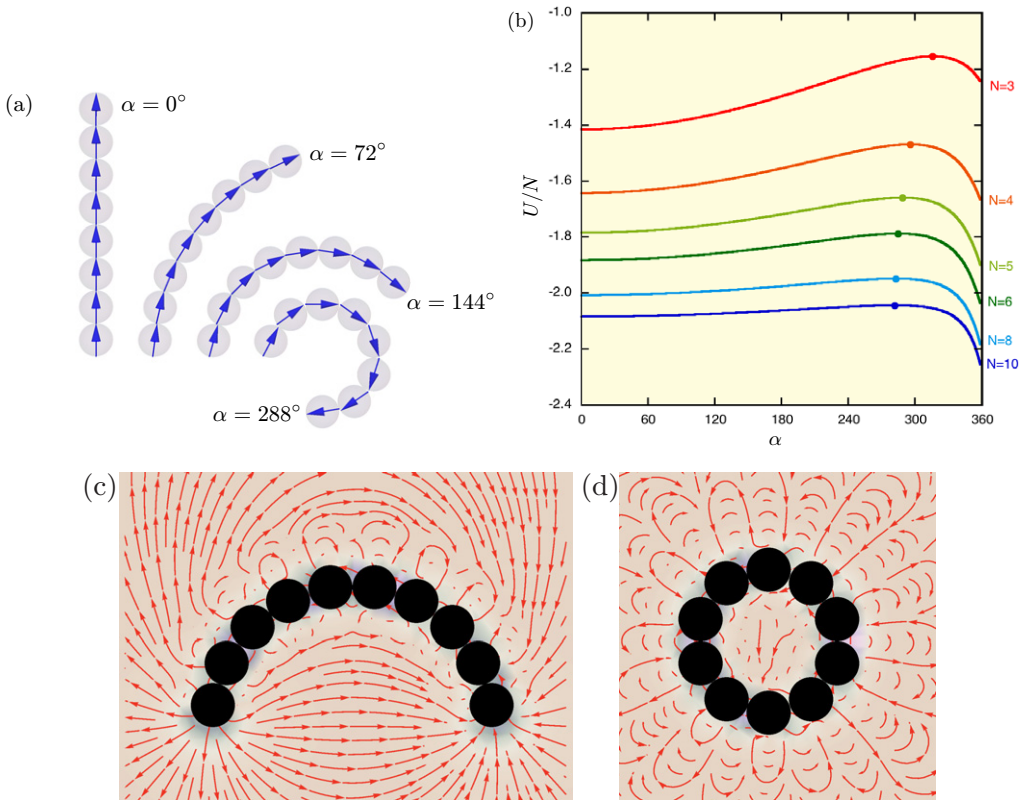

Figure 2. (a) A chain of $N = 8$ dipoles bent from $\alpha = 0$ (line) to $\alpha = 360°$ (closed ring). (b) Energy per particle U/N for a chain continuously bent from 0 to an angle α. Different chain sizes N are illustrated. On each curve, the dot indicates the maximum value giving the barrier position. (c) Field lines around a curved chain of $N = 10$ beads as obtained in numerical simulations: a dipole-like structure is seen, the extremities of the chain being the source and sink of field lines. (d) Field lines around a ring of ten beads. A multipole structure is observed, each sphere being the source and the sink of field lines.

This argument is in favour of a typical distance of interaction and therefore to an increasing angle $\alpha_{\max}$ with N. The fact that a specific angle still exists for large N values underlines that some global properties of the chain emerges, and that subtle long-range phenomena have to be taken into account. It should be also noticed that the bending process from a chain to a ring illustrated in figure 2(a) changes drastically the topology of magnetic field lines at a large scale, i.e. at a scale larger than the magnetized spheres. Two pictures of field lines obtained in our simulations are shown in figures 2(c) and (d), presenting respectively dipole and multipole topologies. In the former case, the long field lines emerge from one chain extremity and sink on the other one whatever the number of spheres. In the ring case, each sphere is the source and sink of field lines. The field line structure evolves therefore from a dipole ($\alpha = 0°$) to a multipole ($\alpha = 360°$) topology. For small α values and long chains, it can be shown that the leading terms of the potential are $U \approx U_0 + \alpha^2/4N + \cdots$ such that any deviation from the rectilinear chain potential is proportional to α^2 (see sections A.1 and A.2 in the appendix). Although the physical origin of this behaviour comes from the dipole–dipole interactions, this quadratic behaviour is shared by elastic systems. This has been recently investigated by Vella *et al* [21]. For a large

number of beads, the chain is more flexible and a small energy input is able to bend the chain to overcome the barrier observed in figure 2. Long chains are therefore forming rings or even 'droplets', as illustrated in figure 3(b). A droplet is generated when one of the chain extremities touches a bead already connected to two neighbours. The reconnection of a chain into a droplet creates a junction where three branches meet. Such a triple junction is the focus of the present paper.

3. Junctions

One observes that the angles formed by the branches at the junction are non-equal. Numerical simulations and experiments show that two angles are identical and larger than 120°, the third one being much smaller. Numerical simulations were performed to estimate those particular angles. Different triple junctions are considered. They are composed of a central bead with three branches each containing L beads for a total bead number $N = 3L + 1$. A variable angle β is considered between a pair of branches. The energy landscapes are shown in figure 3(e) as a function of β between 90° and 150°. Below 90°, unstable configurations are met, while above 150°, beads are overlapping. A minimum of U/N is found for an angle $\beta \approx 143°$, which is in agreement with our experimental observations. The inset of figure 3(e) presents the dipole orientations for that configuration. The central dipole, illustrated in red, is seen to keep the orientation of the central branch.

4. Magnetic ghosts

A triple junction, resulting from a magnetic reconnection, is stable for non-equal angles {143°, 143°, 74°}. Two branches are forming a pair against the third one. By removing the central branch, one expects that the pair of branches will reduce to a simple linear chain. The surprise is that the structure remains in the previous configuration with a similar angle β, keeping the memory of the triple junction! This 'ghost junction' or 'magnetic ghost' is shown in figure 3(c) while a sketch is given in figure 3(f). One should note that gravity is not able to break the ghost junction in figure 3, proving the mechanical stability of the newly formed structure. Figure 3(f) presents the energy per particle for that kind of configuration. A minimum is found for an angle around $\beta \approx 143°$, close to the previous value. The remarkable feature of a ghost junction is that it should be associated to a chain in which dipole orientations suddenly change. For the bead which is the central point of the ghost junction, the dipole keeps the orientation of the branch which has been removed. This frustration should be attributed to a kind of defect between two domains of aligned dipoles. Figure 4(a) presents the field lines around a 'ghost', as obtained in numerical simulations. At the scale smaller than the bead diameter, the dipole nature of the components is observed near the chain. However, at a scale larger than the sphere diameter, the field lines converges towards the frustrated dipole. The latter seems to play the role of a monopole. This will be investigated below. Multiple ghost junctions can be created along a single chain. Zigzags are stable against gravity. If one takes a look at the magnetic field lines at a large scale around the zigzag, as shown in figure 4(b), one discovers that the dipole organization along the zigzag is creating sources and sinks at the defects. Along the chain, the magnetic charges associated to successive ghost junctions have different signs due to the different orientation of the dipoles. Moreover, ghost junctions exhibit long range interactions.

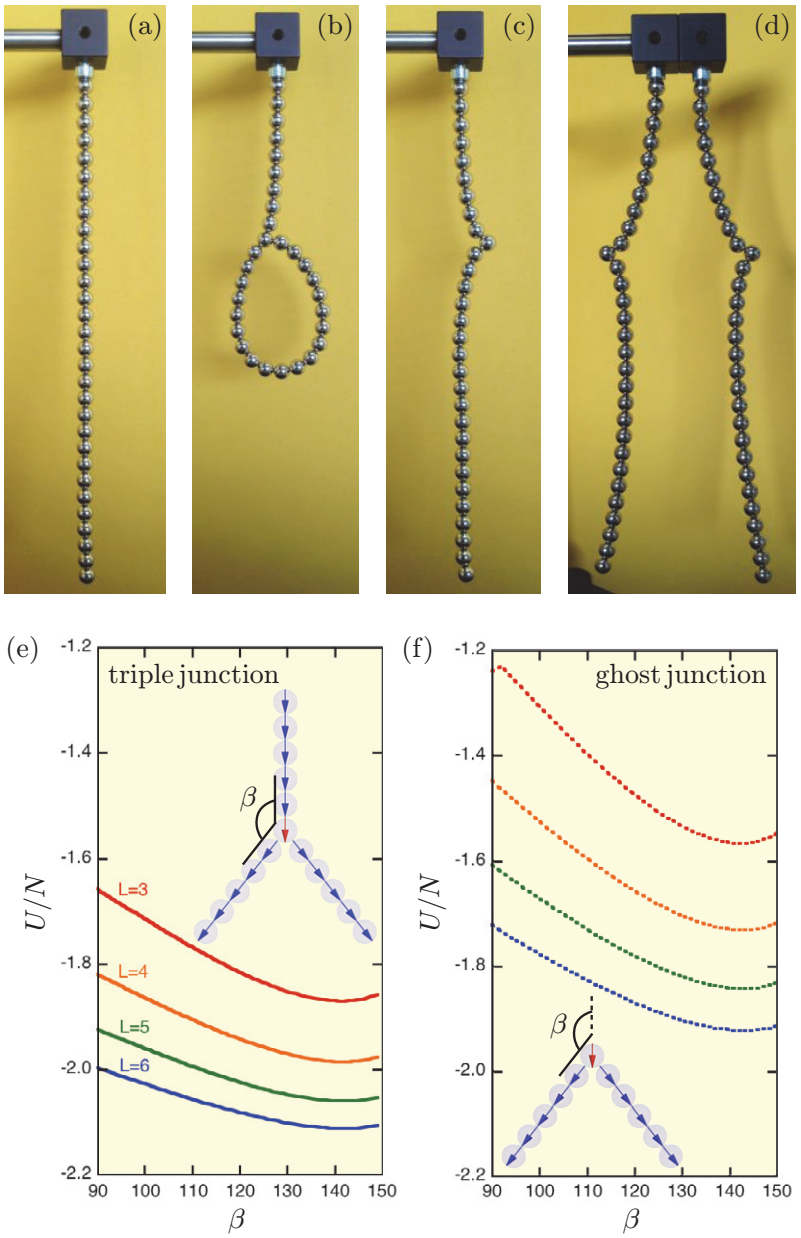

Figure 3. (a) Picture of a vertical chain, made of 30 magnetized spheres, attached at the top and submitted to gravity. (b) Same system forming a 'droplet' due to a magnetic reconnection. (c) Detaching a branch from the triple junction creates a ghost junction for which the memory of the dipole orientation is conserved. (d) Two ghost functions repel each other illustrating the fact that they possess identical magnetic charges. (e) Potential energy U/N as a function of the angle β for a triple junction. Different branch lengths L are illustrated ($N = 3L + 1$). A minimum is obtained for $\beta \approx 143^\circ$. The inset shows a triple junction with non-equal angles minimizing the potential energy from numerical simulations. The red dipole corresponds to the junction itself and the branch length is $L = 5$. (f) Potential energy U/N as a function of the angle β for a ghost junction. Different branch lengths L are illustrated ($N = 2L + 1$). The inset presents the ghost junction minimizing the energy as obtained from numerical simulations.

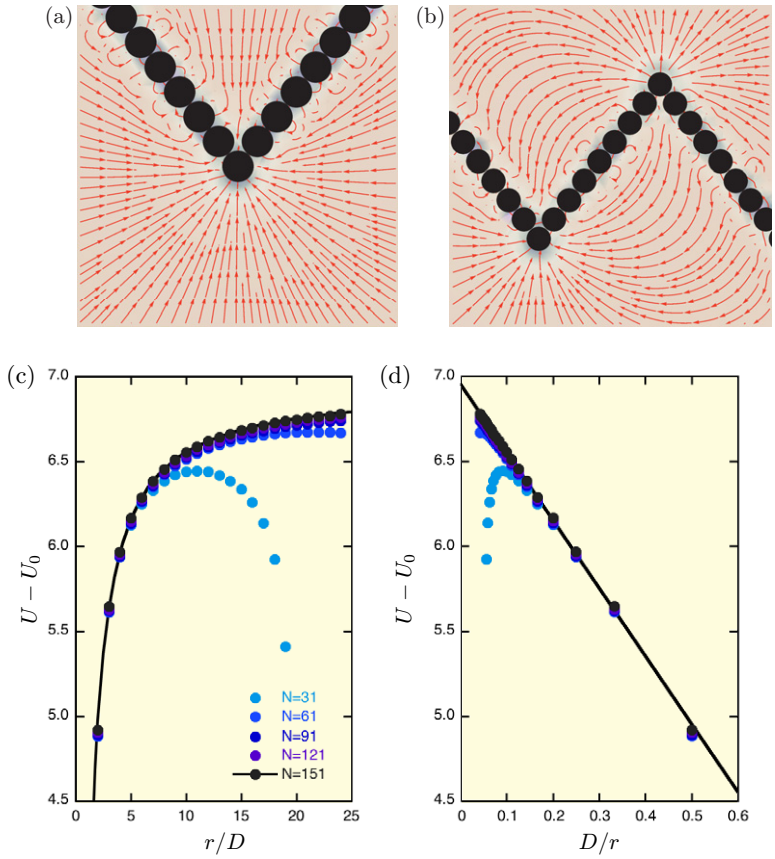

Figure 4. (a) Field lines, as obtained from numerical simulations, around a 'magnetic ghost'. The frustrated dipole behaves like a sink similarity to a monopole. (b) Two defects along a chain which are separated by $r/D = 8$ bead diameters. Field lines seem to emerge from ghost junctions. (c) Dimensionless dipolar energy shifted by the chain energy U_0 for a 1D system containing two 'ghosts' as a function of the distance r between them. Different system sizes are illustrated: $N = \{31, 61, 91, 121, 151\}$. The magnetic Coulomb interaction potential is fitted for the largest system size and is in excellent agreement with the data. (d) Same data as a function of D/r. In this plot, the Coulomb interaction is linear with a unique slope fitted on the data for $N = 151$, providing 'magnetic charge' characteristics and the intercept provides twice the self-energy of a single ghost junction.

Figure 3(d) presents two ghost junctions on two different systems being attached to a support. Gravity orients the systems along the vertical direction. The systems are placed face-to-face for testing the interaction between ghost junctions. Due to their similar magnetic charges, the defects repel each other whatever the initial orientation of the systems. For different dipole orientations, ghosts attract each other, leading to a collapse of the system, not shown in figure 3.

The observation of both attractive and repulsive interactions between ghost junctions motivates a deeper analysis of such systems. Two pseudoparticles A and B, acting as monopoles, are expected to be characterized by the Coulomb-like interaction potential

$$u_{AB} = \frac{\mu_0}{4\pi} \frac{Q_A Q_B}{r_{AB}}, \tag{5}$$

where the magnetic charge Q is given by $Q = \pm m/\xi$ [22]. The length ξ provides a characteristic size for the pseudoparticle. This behaviour has been reported for spin ice systems [22] which are geometrically frustrated ferromagnets on tetrahedral lattices. Spin ice systems lead to a fractionalization of dipoles into monopoles [22].

We studied the energy potential when the dimensionless distance r/D between two ghost junctions is modified. Figure 4(c) shows that dimensionless energy U of the chain as a function of r/D. This energy is shifted by U_0 given by equation (A.1), being the energy of a single chain containing the same number of beads. Different chain sizes are illustrated. For large systems, the interaction between successive defects is attractive and scales as $1/r$: the interaction is remarkably Coulomb-like in between 2 and 25 sphere diameters. The agreement between the fit and the data is excellent. For small systems, finite size effects appear when r/D has the same order of magnitude than N. This generates deviations from the Coulomb law. The same data are shown in figure 4(d) for different chain sizes and as a function of D/r for emphasizing the robustness of the Coulomb-like behaviour. For large N values, all data collapse on the same linear behaviour, meaning that $U - U_0$ measures the energy of the two interacting monopoles. The intercept with the vertical axis gives the self-energy of two isolated ghost junctions. Simulations give a dimensionless self-energy is $U - U_0 \approx 3.45$, close to what is expected from calculations (see section A.3 in the appendix).

From the fit of the data of figures 4(c), (d) with equation (5), taking into account the right units gives $\xi \approx 0.46D$. This particular length should be attributed to the specific angle of the ghost junction and the associated dipole orientations. One should remind that the system is composed of dipoles. It is therefore natural to obtain a characteristic length ξ linked to the dipole size D, above which the system could be regarded as a macroscopic entity. Prior to the present work, spin ice systems were known to show monopoles at the microscopic level. Our observation of stable frustration at the macroscopic scale and for non-equilibrium systems opens ways to explore useful signatures of complex physical phenomena and in particular fractionalization.

We observed that monopoles emerge from a defect in the magnetic structure, exactly like in spin ice systems [22]. From a general point of view, it is interesting to note that the boundary between two ordered domains has a spatial length that is smaller than the elementary magnetic cell, i.e. the size of bead in this case, the distance between two atoms in spin ice. In consequence, the origin of the mechanism for the obtention of monopoles resides in the fractionalization of dipoles at a scale close to the lattice unit, being the bead size here.

5. Summary

In summary, the organization of athermal magnetized spheres leads to a wide variety of structures. We have explored 1D structures such as chains, rings and junctions. By following simple processes such as bending, unexpected mechanically stable structures were discovered. We call them 'ghost junctions' because they keep the memory of a part of the system which has been removed. They seem to act as magnetic monopoles, as demonstrated by field lines and a Coulomb-like interaction.

Since our analysis is only based on dipole–dipole interactions, it is possible to transfer our results to much smaller scales by taking into account thermal agitation. We hope our work will encourage experiments in magnetic dissipative systems like magnetic colloids [2, 3] and magnetic granular systems [15, 16].

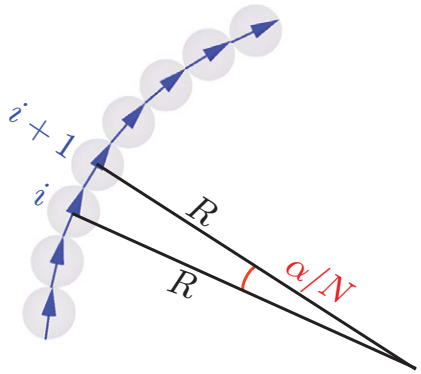

Figure A.1. Sketch of a curved chain with a bending angle α and radius of curvature R.

Acknowledgments

This work is financially supported by the University of Liège (grant no. FSRC-11/36). SD thanks FNRS for financial support. B Vanderheyden and J Martin are acknowledged for fruitful discussions.

Appendix A. Supplementary notes

The following supplementary notes propose to the reader some calculations in order to capture the trends obtained from our numerical simulations. We consider the dimensionless dipole–dipole energies, as proposed in our paper.

A.1. Linear chain

Let us consider a linear chain of N touching spheres. The ground state of the total dipole energy U_0 is obtained when all dipoles are oriented along the chain. One has

$$U_0 = -2\sum_{i=1}^{N-1}\frac{(N-i)}{i^3}. \tag{A.1}$$

This expression is an exact result and should be considered as a basis. When the number of beads increases, the energy per particle U/N tends to

$$\lim_{N\to\infty}\frac{U_0}{N} = -2\zeta(3) \approx -2.4041\ldots. \tag{A.2}$$

A.2. Elastic energy of a curved chain

We assume that the dipoles are tangent to the circular shape of the chain, as shown in figure A.1. The radius of curvature is

$$R = ND/\alpha, \tag{A.3}$$

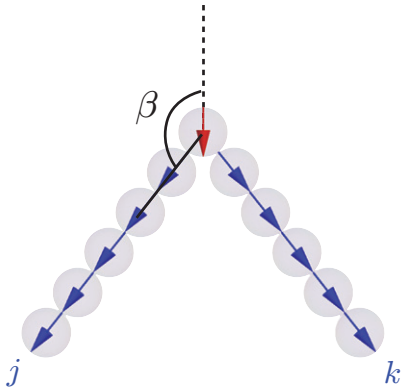

Figure A.2. Sketch of a ghost junction with labels j and k along two branches.

where D is the diameter of the spheres. Taking into account for the curvature of the chain, one can compute the energy of the system, being

$$U = -\frac{1}{2}(N-1)\left[3+\cos\left(\frac{\alpha}{N}\right)\right] - \frac{1}{2}\sum_{i=2}^{N-1}\frac{(N-i)}{i^3}\frac{\left[3+\cos\left(\frac{i\alpha}{N}\right)\right]}{\left[\frac{2N}{i\alpha}\sin\left(\frac{i\alpha}{2N}\right)\right]^3}. \tag{A.4}$$

An energy barrier is obtained from that model. However, some differences remains between our simulation data and this model. Indeed, if one looks carefully at the extremities of a bend chain, dipoles are not particularly following the 'tangent rule' since they tend to be aligned with their unique neighbour. Those effects at the extremities become negligible for large N values.

It is possible to analyse physically the model of equation (2) when the angle α remains small. By developing in series of α/N (first term) and $i\alpha/N$ (other terms), one obtains

$$\begin{aligned} U \approx -\frac{1}{2}(N-1)\left[4-\frac{1}{2}\left(\frac{\alpha}{N}\right)^2+\mathcal{O}\left(\frac{\alpha}{N}\right)^4+\cdots\right] \\ -\frac{1}{2}\sum_{i=2}^{N-1}\frac{(N-\mathrm{i})}{i^3}\left[4+\frac{7}{480}\left(\frac{\mathrm{i}\alpha}{N}\right)^4+\mathcal{O}\left(\frac{\mathrm{i}\alpha}{N}\right)^6+\cdots\right]. \end{aligned} \tag{A.5}$$

The leading terms of the above series are

$$U \approx U_0 + \frac{(N-1)}{4}\left(\frac{\alpha^2}{N^2}\right)+\cdots, \tag{A.6}$$

expressing a parabolic energy increase as a function of α. The chain of dipoles behaves like an elastic material. When the number of beads increases, the elastic constant decreases ($\sim 1/N$) as expected.

A.3. Self-energy of a ghost junction

For the ghost junction, we assume that two chains of length L are connected to a central sphere, as shown in figure A.2. The chains form an angle $2\pi - 2\beta$. The total number of beads is

$N = 2L + 1$. The orientations of the dipoles are assumed to follow the main orientation of their chain. The central magnetic moment is vertical. Taking into account those assumptions, one obtains the dimensionless energy for the ghost junction

$$U = 4\cos\beta \sum_{j=1}^{L} \frac{1}{j^3} - 4\sum_{j=1}^{L-1} \frac{(L-j)}{j^3} + \frac{1}{2}\sum_{j=1}^{L}\sum_{k=1}^{L} \frac{\left[-4(j^2+k^2)\cos 2\beta + jk(7+\cos 4\beta)\right]}{\left(j^2+k^2-2jk\cos 2\beta\right)^{5/2}}, \quad \text{(A.7)}$$

where the first sum corresponds to the interaction of the central sphere with both branches, the second sum is the total energy of spheres interacting only with spheres of their branch, the double sum takes into account the interactions of spheres being placed in different branches. This exact result gives a minimum around $\beta \approx 143^\circ$ that was discussed in the paper.

The difference between U given by the above equation (A.7) and the ground state energy U_0 (from equation (A.1)) can be estimated by numerical means taking the limit of $N \to \infty$. One obtains

$$U - U_0 \approx 3.4517\ldots \quad \text{(A.8)}$$

which represents the self-energy of the ghost junction. The convergence towards this limit is slow ($\sim 1/N$).

References

[1] Kadanoff L P 2000 *Statistical Physics: Statics Dynamics and Renormalization* (Singapore: World Scientific)
[2] Dreyfus R *et al* 2005 *Nature* **436** 862
[3] Zahn K and Maret G 2000 *Phys. Rev. Lett.* **85** 3656
[4] Kun F, Wen W, Pal K F and Tu K N 2001 *Phys. Rev.* E **64** 061503
[5] Wen W, Kun F, Pal K F, Zheng D W and Tu K N 1999 *Phys. Rev.* E **59** R4758
[6] Martin J E 2000 *Phys. Rev.* E **63** 011406
[7] Martin J E, Venturini E, Gulley G L and Williamson J 2004 *Phys. Rev.* E **69** 021508
[8] Whitesides G M and Grzybowski B 2002 *Science* **295** 2418
[9] Pelesko J A 2007 *Self-Assembly* (Boca Raton, FL: Chapman and Hall)
[10] Boncheva M *et al* 2005 *Proc. Natl Acad. Sci. USA* **102** 3924
[11] Snezhko A and Aranson I S 2011 *Nature Mater.* **10** 698
[12] Lumay G, Obara N, Weyer F and Vandewalle N 2013 *Soft Matter* **9** 2420
[13] Snezhko A, Aranson I S and Kwok W K 2005 *Phys. Rev. Lett.* **94** 108002
[14] Vandewalle N, Obara N and Lumay G 2013 *Eur. Phys. J.* E **36** 127
[15] Blair D L and Kudrolli A 2003 *Phys. Rev.* E **67** 021302
[16] Lumay G and Vandewalle N 2007 *New J. Phys.* **9** 406
[17] Carvente O, Peraza-Mues G G, Salazar J M and Ruiz-Suárez J C 2013 *Granular Matter* **14** 303
[18] Falcon E, Bacri J C and Laroche C 2013 *EPL* **103** 64004
[19] Jackson J D 1998 *Classical Electrodynamics* 3rd edn (New York: Wiley)
[20] Rosensweig R E 1997 *Ferrohydrodynamics* (New York: Dover)
[21] Vella D, du Pontavice E, Hall C L and Goriely A 2014 *Proc. R. Soc. Lond.* A **470** 20130609
[22] Castelnovo C, Moessner R and Sondhi S L 2008 *Nature* **451** 42